Soft Matter

PAPER

View Article Online
View Journal | View Issue

Open Access Article. Published on 19 January 2024. Downloaded on 11/20/2025 12:59:55 AM.
This article is licensed under a Creative Commons Attribution 3.0 Unported Licence.

Check for updates

Cite this: *Soft Matter*, 2024, **20**, 1301

Photo-responsive hydrogels based on a ruthenium complex: synthesis and degradation†

Sara Tavakkoli Fard,*[a] Boonya Thongrom,[a] Katharina Achazi,[b] Guoxin Ma,[a] Rainer Haag[a] and C. Christoph Tzschucke*[a]

Received 15th September 2023,
Accepted 26th December 2023

DOI: 10.1039/d3sm01232h

rsc.li/soft-matter-journal

We report the synthesis of a photo responsive metallo-hydrogel based on a ruthenium(II) complex as a functional cross-linker. This metal complex contains reactive 4AAMP (= 4-(acrylamidomethyl)pyridine) ligands, which can be cleaved by light-induced ligand substitution. $Ru[(bpy)_2(4AAMP)_2]$ cross-links 4-arm-PEG-SH macromonomers by thia-Michael-addition to the photocleavable 4AAMP ligand for the preparation of the hydrogel. Irradiation with green light at 529 nm leads to photodegradation of the metallo-hydrogel due to the ligand dissociation, which can be adjusted by adjusting the $Ru[(bpy)_2(4AAMP)_2]$ concentration. The ligand substitution forming $[Ru(bpy)_2(L)_2]^{2+}$ (L = H_2O and CH_3CN) can be monitored by ^1H NMR spectroscopy and UV-visible absorption. The control of degradation by light irradiation plays a significant role in modulating the elasticity and stiffness of the light sensitive metallo-hydrogel network. The photo-responsive hydrogel is a viable substrate for cell cultures.

Introduction

Photo-responsive hydrogels are soft cross-linked materials with particular biocompatibility, biodegradability, physical strength, and chemical properties. Hydrogels have potential applications in biology,[1] medicine[2] and tissue engineering.[3] Since hydrogels are water-swollen polymer networks they are promising substrates for cell cultures due to their ability to mimic the extracellular matrix (ECMs). Using hydrogels to culture cells can support cell adhesion, release active compounds, and influence cell behavior. Additionally, dynamic hydrogel scaffolds can respond to various external stimuli such as temperature[4] light,[1,5] redox-potential,[6] or pH,[7] and influence the cell behavior in ways not feasible in conventional cell culture.[8] Among them, photo-responsive hydrogels are particularly attractive due to their noninvasive and spatiotemporal control abilities. The formation of photo-responsive hydrogels can be achieved by either noncovalent or covalent crosslinking of the hydrogel components. The photodegradation behavior of hydrogels can be controlled by the degree of cross-linking as well as the photo-active component. For different applications, these polymers can be modified with various functional groups.[9] The 3D dimensional structure of hydrogels leads to cell cultures with higher densities and rapid cell growth due to the influence of the adhesivity to cells and elastic modulus compared to standard monolayer culture. Also, the cell viability is enhanced through the attachments to the hydrogel surface.

Different types of light-sensitive crosslinks have been incorporated into polymer networks.[10] For cross-linking most commonly Michael-type addition reactions between the hydrogel components are used. Photoresponsive functional polymers release active compounds under light irradiation with spatio-temporal control. Recently, an amphiphilic block copolymer incorporating ruthenium(II) complexes in the main chain has been investigated as an agent for combined photo-activated chemotherapy and photo-dynamic therapy.[11] Ruthenium complexes among other metal-based complexes have been considered[12,13] because visible light irradiation weakens the ligand-metal bonds of polypyridyl ruthenium complexes. The lowest energy absorption of Ru(II) complexes typically is a metal-to-ligand charge transfer (^{1}MLCT) excitation, which relaxes into a ^{3}MLCT state with high quantum yield. From this long-lived ^{3}MLCT state the low-lying triplet metal-centered (^{3}MC) states, or d–d states, are thermally accessible.[13c,d] This mechanism leads to the ligand photodissociation in ruthenium(II) polypyridyl complexes.[14–16] This behavior is employed in photo-cageing, where a Ru(II) complex is masking a biologically active ligand against interaction with cells. Upon irradiation, a photo-substitution reaction liberates this active ligand. This light-dependent activity of metal complexes offers a very attractive strategy to improve the selective release of photo-responsive ligands at the desired site of biological systems.[17] Through structural design of the ruthenium complex, ligand dissociation in the long wavelength visible light region can be achieved, which allows deep penetration into the desired tissue with fewer side effects.[13,18,19]

[a] *Institut für Chemie und Biochemie, Freie Universität Berlin, Takustraße 3, 14195 Berlin, Germany. E-mail: s.tavakkolifard@yahoo.com, tzschuck@chemie.fu-berlin.de*

[b] *Research Building SupraFAB, Freie Universität Berlin, 14195 Berlin, Germany*

† Electronic supplementary information (ESI) available. See DOI: https://doi.org/10.1039/d3sm01232h

Open Access Article. Published on 19 January 2024. Downloaded on 11/20/2025 12:59:55 AM.
This article is licensed under a Creative Commons Attribution 3.0 Unported Licence.

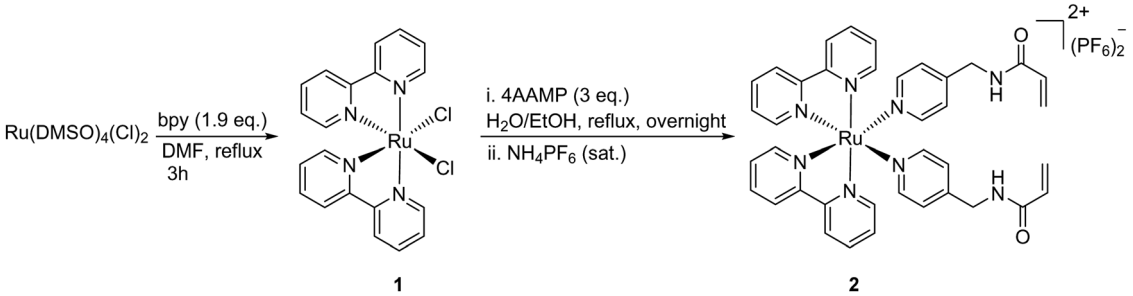

Scheme 1 Synthesis of $[Ru(bpy)_2(4AAMP)_2](PF_6)_2$ **2**.

In this work, the synthesis of the new photo-responsive ruthenium complex based-hydrogel to achieve a photocleavable hydrogel network has been studied. We report the synthesis of a ruthenium complex with photolabile 4-(acrylamidomethyl)-pyridine ligands (4AAMP), which contain a reactive vinyl moiety for further polymer coordination. The photo-responsive ligand 4AAMP was synthesized by introducing an acryloylamide functional group on aminomethyl pyridine (AMP). Then, we prepared ruthenium(II) complex $[Ru(bpy)_2(L_2)](PF_6)_2$ (bpy = 2, 2′-bipyrinine, L = 4AAMP).[20] The photoactivity of Ru(II) complex is attributed to the 4AAMP ligand which can be photo substituted with solvent molecules (CH_3CN and H_2O) at room temperature upon irradiation with green light at 529 nm. Hydrogels were formed by cross-linking 4-arm-PEG-SH macromonomers with the photocleavable 4AAMP ligand on Ru(II) complex by a thia-Michael addition. The photo-responsive hydrogel was employed to culture cells at the surface of hydrogels. The photo-degradation of biocompatible hydrogel leads to the full cleaving of photo-responsive units on the Ru(II) complex which changes viscoelasticity properties over time under light exposure as an external stimulus.

Results and discussion

Synthesis of ruthenium(II) complex

Using previously reported methods,[21] the ligand *N*-(pyridin-4-ylmethyl) acrylamide (4AAMP) was synthesized. This modified amino methyl pyridine (AMP) acts as photocleavable ligand with the acryloyl group as a polymerizable reactive group. The Ru(II) complex **1** was synthesized by a modified procedure starting from $Ru(dmso)_4Cl_2$ and 2,2′-bipyridine (bpy) in DMF at

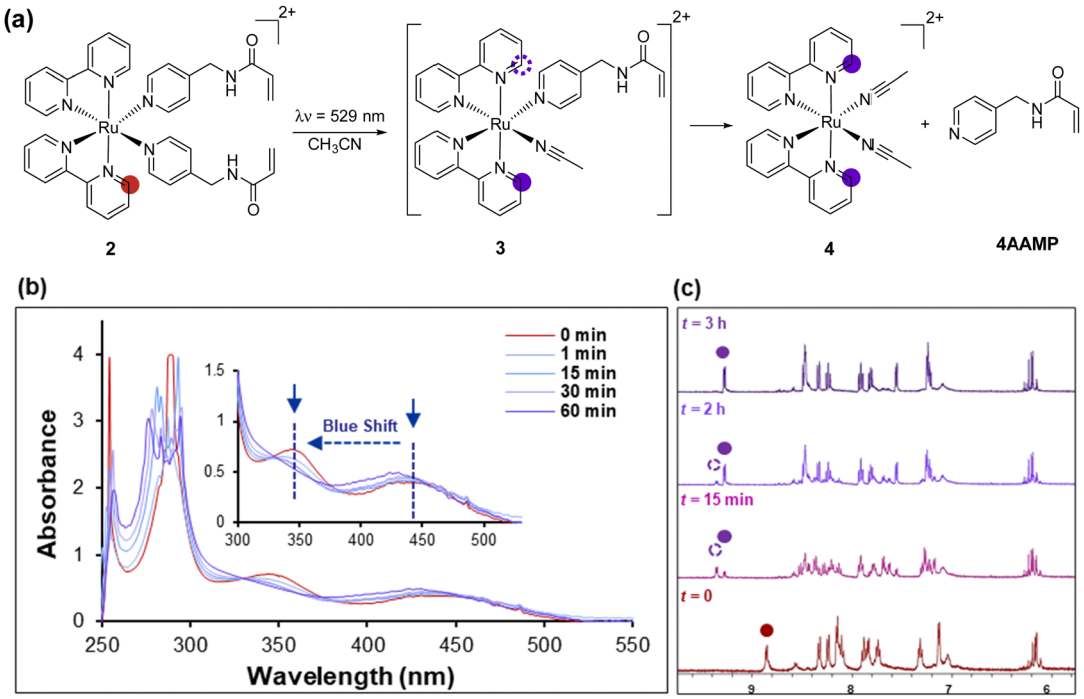

Fig. 1 Photo dissociation of $[Ru(bpy)_2(4AAMP)_2]^{2+}$ in acetonitrile. (a) the proposed photochemical reaction mechanism, (b) evolution of the UV-vis absorption spectra for a solution of $[Ru(bpy)_2(4AAMP)_2]^{2+}$ in H_2O, not irradiated (red line) and upon irradiation with green light, λ = at 529 nm, intensity 28 mW cm^{-2}, 60 min at 25 °C (blue lines), conc. ≈ 7×10^{-5} mol L^{-1}, (c) photochemical reaction was monitored as a function of the irradiation time in 3 h by ^1H NMR spectroscopy in CD_3CN (conc. ≈ 1×10^{-2} mol L^{-1}) at green light, λ = at 529 nm, intensity 28 mW cm^{-2}, 60 min at 25 °C.

Open Access Article. Published on 19 January 2024. Downloaded on 11/20/2025 12:59:55 AM.
This article is licensed under a Creative Commons Attribution 3.0 Unported Licence.

reflux.[22] $[Ru(bpy)_2(4AAMP)_2](PF_6)_2$ **2** was prepared starting from *cis*-$[Ru(bpy)_2Cl_2]$ **1** and 4AAMP in H_2O/EtOH (Scheme 1).[20]

Upon coordination of the 4AAMP ligands to the ruthenium complex the color of the reaction mixture changed from black-purple to orange. The desired complex **2** precipitated after anion exchange with NH_4PF_6 as an orange solid in 95% yield. The synthesis and workup of this reaction was performed under reduced light. ^{1}H and ^{13}C NMR spectroscopy and mass spectrometry were consistent with the structure of the compound. UV/Vis absorption spectra of $[Ru(bpy)_2(4AAMP)_2](PF_6)_2$ **2** were measured in water (conc. $\approx 7 \times 10^{-5}$ mol L^{-1}) (Fig. 1a). Ruthenium complex **2** displays a broad absorption band at 450 nm owing to the metal-to-ligand charge transfer (MLCT) transition band.[19d,23] The signals at around 290 nm and 350 nm indicate the π–π* transitions of the bipyridine ligands (Fig. 1b). The photo-substitution of the 4AAMP ligand by acetonitrile or water upon irradiation at 529 nm, shifted the signal of the MLCT band at 450 nm to a shorter wavelength of 430 nm.[20a] The first rapid ligand substitution occurs during approximately 1 min of light irradiation, and converts $[Ru(bpy)_2(4AAMP)_2]^{2+}$ to $[Ru(bpy)_2(4AAMP)(H_2O)]^{2+}$ **3b** (Fig. S16a, ESI†), replacing one 4AAMP ligand by H_2O. Because of the slow photo-substitution of the second 4AAMP after 1 hour, it is suggested that an isosbestic point at around 390 nm disappears. The second isosbestic point at 370 nm is attributed to the second 4AAMP ligand dissociation and the formation of the photo product complex $[Ru(bpy)_2(H_2O)_2]^{2+}$ **4b** (Fig. S16a, ESI†).[20a] These particular changes in the absorption spectra suggest that the photo substitution of ruthenium complex **2** was completed within 1 hour and takes place in two steps upon irradiation with green light. (Fig. 1a). In order to explain these photoreaction differences, the dissociation of the photocleavable ligands from $[Ru(bpy)_2(4AAMP)_2]^{2+}$ **2** in CD_3CN was monitored by ^{1}H NMR spectroscopy under green light irradiation during 3 hours (Fig. 1c).

The signal at 8.9 ppm of the non-irradiated complex $[Ru(bpy)_2(4AAMP)_2]^{2+}$ **2** disappeared and a new signal at 9.3 ppm appeared after 3 h irradiation, which we interpret as result of the efficient substitution of the 4AAMP-ligands by acetonitrile. The signal at 9.3 ppm is assigned to the *ortho*-protons of the bipyridine which indicates the formation of two different photo species, complexes **3** and **4**, with different signals at 9.3 and 9.4 ppm within 15 min irradiation.

Metallo-hydrogel formation

Formation of a photo responsive metallo-hydrogel was achieved by connecting $[Ru(bpy)_2(4AAMP)_2]^{2+}$ through the nucleophilic thiol-en Michael addition reaction with 4-arm poly(ethylene glycol) thiol (4-arm-PEG-SH, M_w = 10 kDa) in phosphate buffer saline solution (PBS, pH = 7.2) at 37 °C. (Fig. 2). The thiol functional group on 4-arm-PEG-SH and the electron-deficient acryloyl C–C double-bonds on the Ru(II) complex enable S–C bond formation and the desired crosslinks under mild reaction conditions.[23b] To study the influence of the degree of cross-linking, photo responsive metallo-hydrogels with different ratios of gel components Ru(II) and 4-arm-PEG-SH were synthesized with gel concentrations from 2 to 10% (*w*/*v*) (Table S1, ESI†). Decreasing the gel concentration results in decreasing in the number of crosslinks, thus, gel viscosity decreased and a more liquid and softer gel was obtained. A molar ratio of the Ru(II) to 4-arm-PEG10k-SH (AAMP: SH) of 2 : 1 resulted in a more elastic gel than a molar ratio of the components of 1.5 : 1. Accordingly, a concentration of 2% (w/v) with a 1.5 : 1 mmol ratio of the components generated the softest hydrogel. Also there is a clear physical difference between two series of hydrogels. At the highest concentration of 10% (w/v) and a

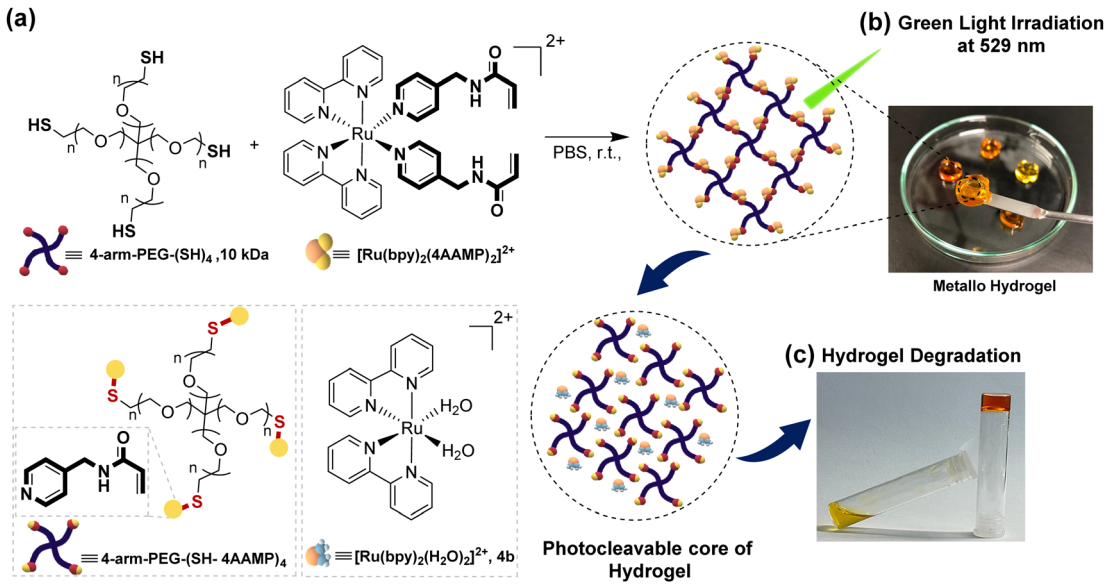

Fig. 2 (a) Schematic representation of the metallo-hydrogel synthesis, (b) a cartoon representation of hydrogel degradation under exposure of green light at 529 nm, (c) The degradation reaction and image has been taken from the sample 2% (w/v) under exposure of light.

Open Access Article. Published on 19 January 2024. Downloaded on 11/20/2025 12:59:55 AM.
This article is licensed under a Creative Commons Attribution 3.0 Unported Licence.

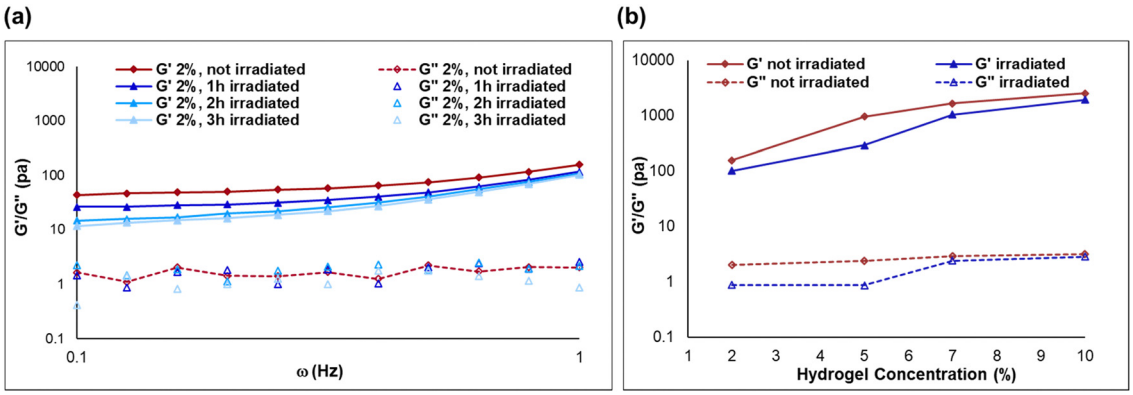

Fig. 3 Rheological characterization of hydrogel under the green light-induced degradation reaction within 3 hours at 529 nm, intensity 28 mW cm^{-2}; Storage (G') and loss (G'') moduli as a function of radial frequency (ω = 0.1–10 Hz). (a) 2% (w/v) gels, and (b) comparisons between 2, 5, 7 and 10% (w/v) hydrogels for samples in which the gel component ratio is 1.5 : 1 of [Ru] complex/PEG 4 arm thiol at 25 °C, frequency (ω = 0.1–10 Hz) upon 3 h irradiation.

2 : 1 molar ratio of the components, the orange clear solution rapidly converted to a solid hydrogel with the highest elasticity. The physical properties and degradation behavior of the hydrogels were characterized by rheological experiments under light irradiation during 3 hours (Fig. 3a). Which resulted in the irradiation time dependent shear modulus or viscoelasticity (G'/G'') value that are related to the viscous and elastic response behavior of the hydrogel. The degradation of the hydrogel under green light irradiation at 529 nm occurs, because the 4AAMP ligands are substituted with water which effectively cleaves the cross-links and forms photoproduct $[Ru(bpy)_2(H_2O)_2]^{2+}$ **4b** (Fig. 2 and Fig. S16a, ESI†). The hydrogel with 2% (w/v) and 1.5 : 1 mmol ratio of components showed the fastest degradation as indicated by the drop in storage modulus (G') and loss modulus (G'') which leads to a low viscose liquid after light exposure (Fig. 3a).

The metallo-hydrogels with a 1.5 : 1 molar ratio of Ru(II)-complex to 4-arm-PEG-SH show an increase in elasticity and viscosity with increasing gel concentration from 2% to 10% (w/v) (Fig. 3b). Also, these hydrogels showed a drop of storage module G' after a specific strain under light irradiation (Fig. 3b and Fig. S20–S23, ESI†). The hydrogels with 2% or 5% concentration are degraded significantly faster under irradiation than the ones with 7% or 10%. The mesh

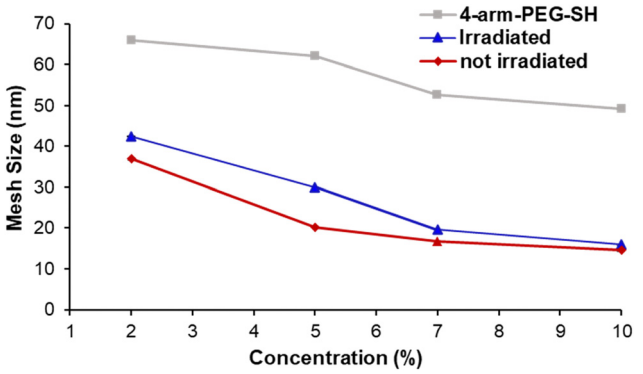

Fig. 4 Mesh size, which is calculated by the storage modulus at 1 Hz from frequency sweep test at 25 °C, of different concentration of hydrogels before and after degradation for 2, 5, 7 and 10% (w/v) hydrogels.

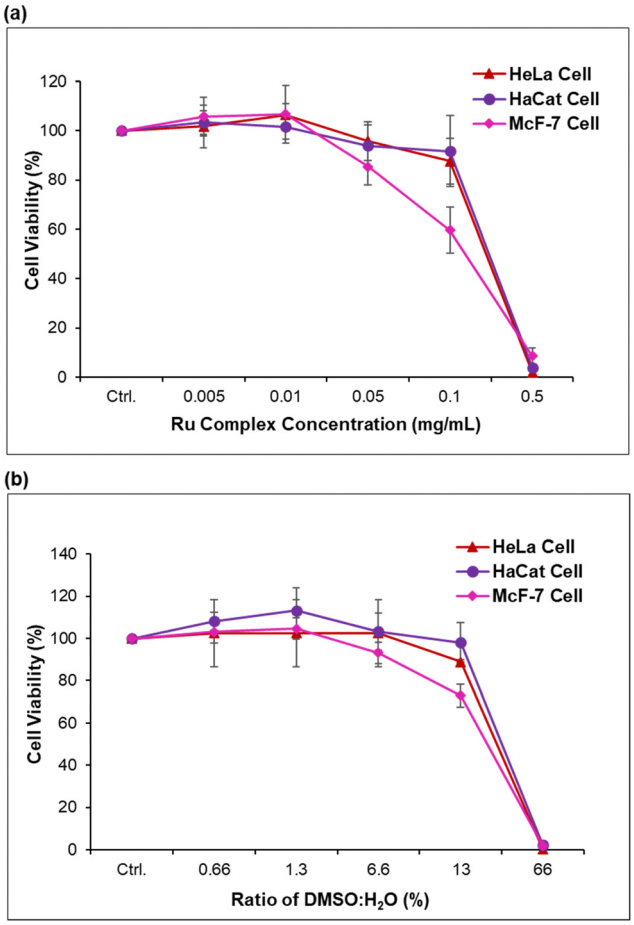

Fig. 5 (a) MTT cell viability assay of photoproducts after photo dissociation of $[Ru(bpy)_2(4AAMP)_2]^{2+}$ in water under green light (529 nm, 28 mW cm^{-2}) for 1 h was performed for HeLa, McF-7 and HaCat cell lines after 48 h incubation time; the Ru(II) complex (10 mg mL^{-1}) was added as solution in DMSO: H_2O (66%); (b) MTT cell viability assay a solution of DMSO: H_2O for HeLa, McF-7 and HaCat cell lines after 48 h incubation time.

Open Access Article. Published on 19 January 2024. Downloaded on 11/20/2025 12:59:55 AM.
This article is licensed under a Creative Commons Attribution 3.0 Unported Licence.

size of the metallo-hydrogels, at concentrations ranging from 2 to 10% (w/v) and a 1.5 : 1 molar ratio, was determined using the storage modulus value (G') obtained from the oscillatory frequency sweep test at 1 Hz, as illustrated in Fig. 3. As anticipated, the stiffening effect of the 2% hydrogel was observed, confirming higher stiffness properties associated with an increase in the mesh size under light irradiation (Fig. 4). Hence, the softer 2% hydrogel due to its higher water content, and notably its ability to readily liquefy within 3 hours of irradiation is appropriate for the following cell culture experiments. The mesh size was calculated using the classical theory of rubber elasticity, as outlined below:[24]

$$r = \left(\frac{6RT}{\pi N_{AV} G}\right)^{1/3}$$

where r is mesh size (nm), R is the universal gas constant (8.314 J K^{-1} mol^{-1}), T is temperature (K), π is Archimede's constant (3.141...), N_{AV} is Avogadro's number (6.022×10^{23} mol^{-1}), and G is the storage shear modulus (Pa).

In vitro degradation assay

To assess the biocompatibility of the hydrogels, first the cytotoxicity of the new Ru(II) complex **2** was tested against three different cells types (HeLa, HaCaT and McF-7) with and without green light irradiation. $[Ru(bpy)_2(4AAMP)_2]^{2+}$ **2** did not show any significant cytotoxicity in the dark or under green light exposure (529 nm, 28 mW cm^{-2}) (Fig. 5a and Fig. S25, ESI†), and toxicity increased only at concentrations ≥ 0.5 μg mL^{-1}. In particular, the cytotoxicity was not higher than for the control with only the solution of DMSO:H_2O (Fig. 5b). Therefore, we assumed that the hydrogels derived from complex **2** would be biocompatible, because the final concentration of ruthenium complex in the hydrogels would be less than 0.05 mg mL^{-1}. To test this assumption, we investigated cell adhesion on the hydrogel, conditions for settling and seeding cells on its

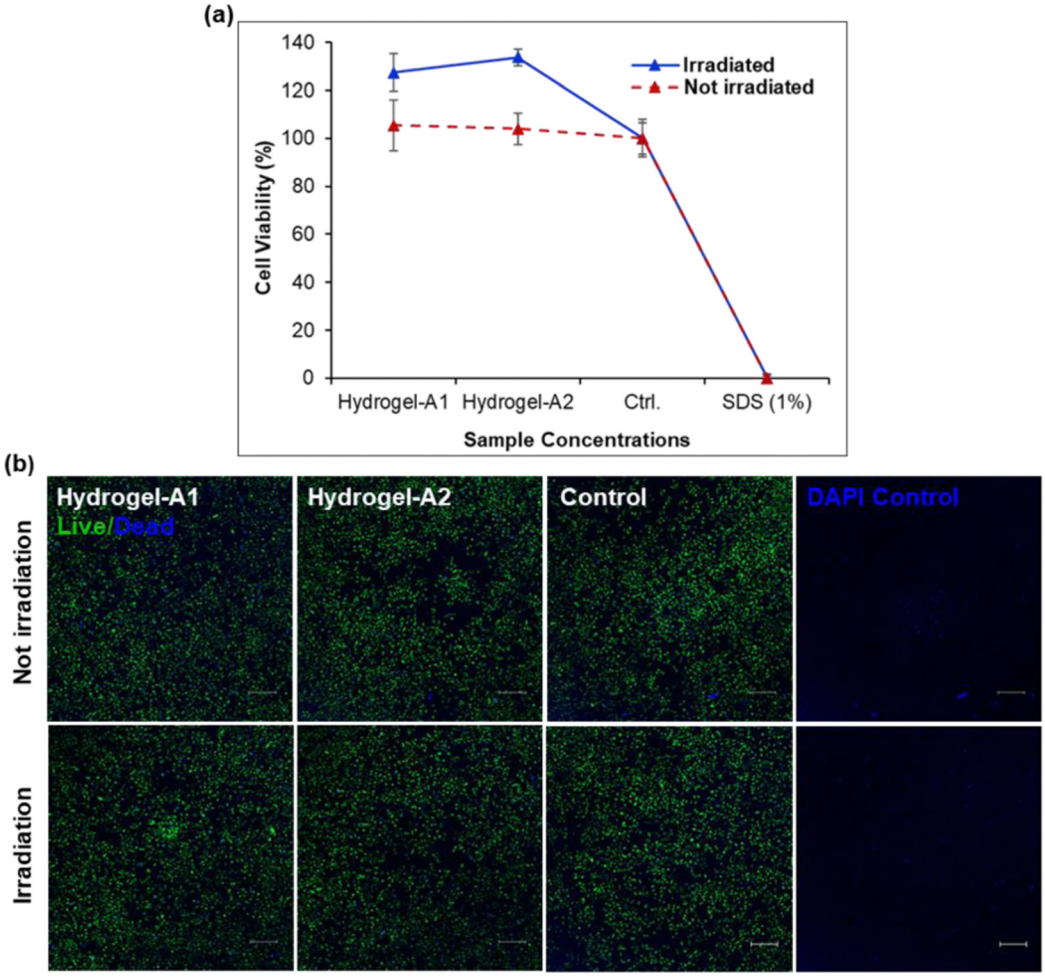

Fig. 6 (a) MTT cell viability assay of metallo hydrogel-A1 and A2 (1.5 and 2 molar ratio of Ru(II) to 4-arm-PEG10k-SH (AAMP: SH), respectively) in DMEM medium, without irradiation and after irradiation for 1 h; (b) confocal microscopy overlay images of GFP HeLa cells cultured on the metallo hydrogel 2% metallo hydrogel-A1 and A2 1.5 and 2 molar ratio of Ru(II) to 4-arm-PEG10k-SH (AAMP: SH) and counter staining was performed using DAPI (0.5 μM for 10 min) to visualize the nucleus DAPI λ_{em} = 461 nm, λ_{ex} = 353 nm, GFP λ_{em}= 509, λ_{ex} = 395 nm, nm, Object: 5x, Inset scale bars: 250 μm, irradiation time: 1 h under light irradiation (529 nm, 28 mW cm^{-2}).

Open Access Article. Published on 19 January 2024. Downloaded on 11/20/2025 12:59:55 AM.
This article is licensed under a Creative Commons Attribution 3.0 Unported Licence.

surface, and the impact of the hydrogel's mechanical properties after degradation during cell cultures. First the biocompatibility of the hydrogel was investigated quantitively with an MTT cell viability assay using the GFP HeLa cell line (Fig. 6a). For this assay, hydrogel samples Hydrogel-A1 and Hydrogel-A2, each with a final gel concentration of 2% (w/v) and a 1.5 or 2 molar ratio of Ru(II) complex **2** to 4-arm-PEG-SH, respectively, were prepared in a 96-cell well plate. In this experiment, Ru complex was dissolved in PBS at a concentration of 1 mg/mL to avoid using DMSO. After 1 day, DMEM medium was added to all hydrogel samples. The following day, the hydrogel degradation was induced by irradiating with LED green light for approximately 1 hour. The supernatant, consisting of DMEM, was collected, added to the top of cells in another 96-well plate, and incubated over night at 37 °C. MTT assay was conducted after 1 day of seeding cells with different hydrogel supernatants, including a control. The results after 3 h incubation with CCK8 showed a cell viability of 105 ± 8% for Hydrogel-A1 and 104 ± 3.5% for Hydrogel-A2 (Fig. 6a). The cell viability appeared to be higher for both hydrogels after irradiation and compared to the control without gel. We hypothesize that photoproducts of the gel degradation with an absorbance at 460 nm, where also CCK8 is detected, are responsible for this artefact. Additionally, a live/dead cell assay was conducted using GFP HeLa cells after 1 day of culture on the hydrogels (Fig. 6b and Fig. S27a, ESI†). To visualize the differential potential of seeding HeLa cells on a metallo-hydrogel, a μ-slide 15 well 3D with specialized geometry was employed to prepare a uniformly thick gel matrix for reproducible formation assays. The cells were seeded on top of the hydrogels in the μ-slide. After incubation for 24 h, the photo-responsive hydrogels were degraded by light irradiation for 1 h. As depicted in Fig. 6b, cells attached well and adopted spindle or polyhedron shapes at the surface of both gels. The growth of cells on the hydrogel was then compared to the control which displayed a similar viability of HeLa cell. The intensity of the GFP green color indicated a similar density of live cells in hydrogels with control, the total percentages of dead cells, approximately was determined using image analysis tool, Fiji[25] in the samples, by 2% in Hydrogel-A1, 3% in Hydrogel-A2 and the control. And cells were able to grow and spread even after irradiation, showing no significant difference in cell viability between the control and the metal-containing hydrogels (Fig. 6b). Following gel degradation, cells began assuming circular shapes and started the formation of colonies on the hydrogel. The uniform distribution patterns of HeLa cells on the metallo-hydrogel resembled the distribution on the control. Despite the decrease in elasticity and viscosity after irradiation, it appears that cell viability did not significantly reduce after this change in the morphology of the gels. The quantitation approach of the image data for dead cells presented a 4% rate in Hydrogel-A2 compared to 3% in Hydrogel-A1 and 3.5% in the control. It is also possible that cells penetrated into the matrix of the hydrogel, not solely remaining on the surface.

To the best of our knowledge, this seeding method on the metal-containing hydrogels has not been reported in other studies. Here, for the first time, we demonstrate that metallo-hydrogels can provide a biocompatible environment to grow cells with enough attachment on metallo hydrogel, similar to seeding in the 2D method. Notably, the softer Hydrogel-A1 is suitable for culturing different cell lines, while the other, stiffer Hydrogel-A2 with a larger molar ratios of gel components is less favorable and has shown different viability and growth patterns in gel cultures compared to the conventional culture methods.

Conclusion

A new photo-responsive $[Ru(bpy)_2(4AAMP)_2]^{2+}$ complex **2** was developed as a building-block for light sensitive soft materials for biological studies. Ruthenium complex **2** with the photo-cleavable monodentate ligand 4AAMP was coupled with 4-arm-PEG-SH to prepare a photosensitive metallo-hydrogel scaffold. Further, it was demonstrated that establishing mechanical control is possible by altering the concentration or ratio of Ru(II) complex as a cross-linking. In addition, the highly hydrate hydrogel with an aqueous phase and low degree of cross-linking might be suitable platform technology to cell culture support, because of the small time and energy input needed to modify the hydrogel stiffness. The application of system provide a suitable biocompatible environment to growth cells with spatiotemporal control of cell support elasticity. Which provides a way to study the influence of stiffness and elasticity of the hydrogel on cell behavior. Since metallo-hydrogels are easy to process, they could become a unique platform to support the growth of cells.

Conflicts of interest

The authors declare no conflict of interest.

Acknowledgements

The authors gratefully acknowledge Collaborative Research Center SFB1449 for financial support. Also, we would like to thank the core-facility BioSupraMol of the Freie Universität Berlin for the analytical support. Furthermore, we thank Elisa Quaas for technical assistance in the biological laboratory.

References

1 H. Zhu, H. Yang, Y. Ma, T. J. Lu, F. Xu, G. M. Genin and M. Lin, *Adv. Funct. Mater.*, 2020, **30**, 2000639.
2 (*a*) S. Koutsopoulos, L. D. Unsworth, Y. Nagai and S. Zhang, *Proc. Natl. Acad. Sci. U. S. A.*, 2009, **106**, 4623–4628; (*b*) S. J. Bhuniya, Y. J. Seo and B. H. Kim, *Tetrahedron Lett.*, 2006, **47**, 7153–7156; (*c*) S. Sutton, N. L. Campbell, A. I. Cooper, M. Kirkland, W. J. Frith and D. J. Adams, *Langmuir*, 2009, **25**, 10285–10291.
3 (*a*) M. C. Branco, D. J. Pochan, N. J. Wagner and J. P. Schneider, *Biomaterials*, 2010, **31**, 9527–9534; (*b*) E. Genove, C. Shen, S. G. Zhang and C. E. Semino, *Biomaterials*, 2005, **26**, 3341–3351; (*c*) J. P. Jung, A. K. Nagaraj,

 This journal is © The Royal Society of Chemistry 2024

Open Access Article. Published on 19 January 2024. Downloaded on 11/20/2025 12:59:55 AM.
This article is licensed under a Creative Commons Attribution 3.0 Unported Licence.

E. K. Fox, J. S. Rudra, J. M. Devgun and J. H. Collier, *Biomaterials*, 2009, **30**, 2400–2410.

4 (*a*) C. Wang, R. J. Stewart and J. Kopecek, *Nature*, 1999, **397**, 417; (*b*) K. Trabbic-Carlson, L. A. Setton and A. Chilkoti, *Biomacromolecules*, 2003, **4**, 572–580.

5 (*a*) J. Huang and A. Heise, *Chem. Soc. Rev.*, 2013, **42**, 7373–7390; (*b*) Y. Shen, X. Fu, W. Fu and Z. Li, *Chem. Soc. Rev.*, 2015, **44**, 612–622; (*c*) H. Yao, J. Wang and S. Mi, *Polymers*, 2018, **10**, 11; (*d*) B. P. Purcell, D. Lobb, M. B. Charati, S. M. Dorsey, R. J. Wade, K. N. Zellars, H. Doviak, S. Pettaway, C. B. Logdon and J. A. Shuman, *Nat. Mater.*, 2014, **13**, 653; (*e*) M. F. Maitz, U. Freudenberg, M. V. Tsurkan, M. Fischer, T. Beyrich and C. Werner, *Nat. Commun.*, 2013, **4**, 2168; (*f*) M. Nakahata, Y. Takashima, H. Yamaguchi and A. Harada, *Nat. Commun.*, 2011, **2**, 511; (*g*) S.-J. Jeon, A. W. Hauser and R. C. Hayward, *Acc. Chem. Res.*, 2017, **50**, 161.

6 (*a*) X. Z. Shu, Y. Liu, F. Palumbo and G. D. Prestwich, *Biomaterials*, 2003, **24**, 3825–3834; (*b*) W. Shen, R. G. H. Lammertink, J. K. Sakata, J. A. Kornfield and D. A. Tirrell, *Macromolecules*, 2005, **38**, 3909–3916; (*c*) N. Kong, Q. Peng and H. Li, *Adv. Funct. Mater.*, 2014, **24**, 7310–7317.

7 G. Zabow, S. J. Dodd and A. P. Koretsky, *Nature*, 2015, **529**, 73–77.

8 (*a*) B. M. Baker and C. S. Chen, *J. Cell Sci.*, 2012, **125**, 3015–3024; (*b*) M. P. Lutolf and J. A. Hubbell, *Nat. Biotechnol.*, 2005, **23**, 47–55.

9 (*a*) L. Li, J. M. Scheiger and P. A. Levkin, *Adv. Mater.*, 2019, **31**, 1807333; (*b*) X. B. Zhao, F. Pan, H. Xu, M. Yaseen, H. H. Shan, C. A. E. Hauser, S. G. Zhang and J. R. Lu, *Chem. Soc. Rev.*, 2010, **39**, 3480–3498; (*c*) F. Gelain, A. Horii and S. G. Zhang, *Macromol. Biosci.*, 2007, **7**, 544–551; (*d*) G. A. Silva, C. Czeisler, K. L. Niece, E. Beniash, D. A. Harrington, J. A. Kessler and S. I. Stupp, *Science*, 2004, **303**, 1352–1355; (*e*) K. M. Galler, L. Aulisa, K. R. Regan, R. N. D'Souza and J. D. J. Hartgerink, *J. Am. Chem. Soc.*, 2010, **132**, 3217–3223; (*f*) E. L. Bakota, Y. Wang, F. R. Danesh and J. D. Hartgerink, *Biomacromolecules*, 2011, **12**, 1651–1657; (*g*) M. Zhou, A. M. Smith, A. K. Das, N. W. Hodson, R. F. Collins, R. V. Ulijn and J. E. Gough, *Biomaterials*, 2009, **30**, 2523–2530; (*h*) J. P. Jung, J. Z. Gasiorowski and J. H. Collier, *Biopolymers*, 2010, **94**, 49–59.

10 (*a*) I. Tomatsu, K. Peng and A. Kros, *Adv. Drug Delivery Rev.*, 2011, **63**, 1257–1266; (*b*) M. B. Charati, I. Lee, K. C. Hribar and J. A. Burdick, *Small*, 2010, **6**, 1608–1611; (*c*) C. de Gracia Lux, J. Lux, G. Collet, S. He, M. Chan, J. Olejniczak, A. Foucault-Collet and A. Almutairi, *Biomacromolecules*, 2015, **16**, 3286–3296.

11 (*a*) W. Sun, S. Li, B. Häupler, J. Liu, S. Jin, W. Steffen, U. S. Schubert, H.-J. Butt, X.-J. Liang and S. Wu, *Adv. Mater.*, 2017, **29**, 1603702; (*b*) I. Teasdale, S. Theis, A. Iturmendi, M. Strobel, S. Hild, J. Jacak, P. Mayrhofer and U. Monkowius, *Chem. Eur. J.*, 2019, **25**, 9851–9855; (*c*) S. Bonnet, *J. Am. Chem. Soc.*, 2023, **145**, 23397–23415.

12 (*a*) S. Bonnet, *Dalton Trans.*, 2018, **47**, 10330–10343; (*b*) N. L. Salassa and P. Sadler, *J. Dalton Trans.*, 2009, **38**, 10690–10701; (*c*) W. A. Velema, W. Szymanski and B. L. Feringa, *J. Am. Chem. Soc.*, 2014, **136**, 2178–2191; (*d*) S. Gai, G. Yang, P. Yang, F. He, J. Lin, D. Jin and B. Xing, *Nano Today*, 2018, **19**, 146–187; (*e*) C. Mari, V. Pierroz, S. Ferrari and G. Gasser, *Chem. Sci.*, 2015, **6**, 2660–2686; (*f*) B. A. Albani, B. Pena, N. A. Leed, N. A. de Paula, C. Pavani, M. S. Baptista, K. R. Dunbar and C. Turro, *J. Am. Chem. Soc.*, 2014, **136**, 17095–17101.

13 (*a*) S. Dilruba and G. V. Kalayda, *Pharmacological*, 2016, **77**, 1103–1124; (*b*) D. Lebwohl and R. Canetta, *Eur. J. Cancer*, 1998, **34**, 1522–1534; (*c*) S. Bonnet, *Dalton Trans.*, 2018, **47**, 10330–10343; (*d*) C. Yongjie, B. Lijuan, Z. Pu, Z. Hua and Z. Qianxiong, *Molecules*, 2021, **26**, 5679.

14 (*a*) O. Filevich and R. Etchenique, *Photochem. Photobiol. Sci.*, 2013, **12**, 1565–1570; (*b*) N. J. Farrer, L. Salassa and P. J. Sadler, *Dalton Trans.*, 2009, 10690–10701; (*c*) U. Schatzschneider, *Eur. J. Inorg. Chem.*, 2010, 1451–1467.

15 (*a*) X.-H. Qin, X. Wang, M. Rottmar, B. J. Nelson and K. Maniura-Weber, *Adv. Mater.*, 2018, **30**, 1705564; (*b*) J. A. Peterson, C. Wijesooriya, E. J. Gehrmann, K. M. Mahoney, P. P. Goswami, T. R. Albright, A. Syed, A. S. Dutton, E. A. Smith and A. H. Winter, *J. Am. Chem. Soc.*, 2018, **140**, 7343–7346; (*c*) P. Xiao, J. Zhang, J. Zhao and M. H. Stenzel, *Prog. Polym. Sci.*, 2017, **74**, 1–33; (*d*) J. T. Offenloch, M. Gernhard, J. P. Blinco, H. Frisch, H. Mutlu and C. Barner-Kowollik, *Chem. – Eur. J.*, 2019, **25**, 3700–3709.

16 (*a*) B. Guo and P. X. Ma, *Sci. China: Chem.*, 2014, **57**, 490–500; (*b*) D. Y. Wong, D. R. Griffin, J. Reed and A. M. Kasko, *Macromolecules*, 2010, **43**, 2824–2831; (*c*) C. de Gracia Lux, C. L. McFearin, S. Joshi-Barr, J. Sankaranarayanan, N. Fomina and A. Almutairi, *ACS Macro Lett.*, 2012, **1**, 922–926; (*d*) A. Ovsianikov, V. Mironov, J. Stampfl and R. Liska, *Expert Rev. Med. Devices*, 2012, **9**, 613–633.

17 (*a*) J.-A. Cuello-Garibo, M. S. Meijer and S. Bonnet, *Chem. Commun.*, 2017, **53**, 6768–6771; (*b*) D. F. Azar, H. Audi, S. Farhat, M. El-Sibai, R. J. Abi-Habib and R. S. Khnayzer, *Dalton Trans.*, 2017, **46**, 11529–11532; (*c*) L. Zayat, C. Calero, P. Albores, L. Baraldo and R. Etchenique, *J. Am. Chem. Soc.*, 2003, **125**, 882–883; (*d*) B. S. Howerton, D. K. Heidary and E. C. Glazer, *J. Am. Chem. Soc.*, 2012, **134**, 8324–8327.

18 (*a*) S. L. Hopkins, B. Siewert, S. H. C. Askes, P. Veldhuizen, R. Zwier, M. Heger and S. Bonnet, *Photochem. Photobiol. Sci.*, 2016, **15**, 644–653; (*b*) A. N. Bashkatov, E. A. Genina, V. I. Kochubey and V. V. Tuchin, *J. Phys. D: Appl. Phys.*, 2005, **38**, 2543–2555.

19 (*a*) A. Li, R. Yadav, J. K. White, M. K. Herroon, B. P. Callahan, I. Podgorski, C. Turro, E. E. Scott and J. Kodanko, *J. Chem. Commun.*, 2017, **53**, 3673–3676; (*b*) A.-C. Laemmel, J.-P. Collin and J.-P. Sauvage, *Eur. J. Inorg. Chem.*, 1999, 383–386; (*c*) Q. Sun, S. Mosquera-Vazquez, L. M. Lawson Daku, L. Guenee, H. A. Goodwin, E. Vauthey and A. Hauser, *J. Am. Chem. Soc.*, 2013, **135**, 13660–13663; (*d*) E. Wachter, D. K. Heidary, B. S. Howerton, S. Parkin and E. C. Glazer, *Chem. Commun.*, 2012, **48**, 9649–9651; (*e*) B. S. Howerton, D. K. Heidary and E. C. Glazer, *J. Am. Chem. Soc.*, 2012, **134**, 8324–8327.

Open Access Article. Published on 19 January 2024. Downloaded on 11/20/2025 12:59:55 AM.
This article is licensed under a Creative Commons Attribution 3.0 Unported Licence.

20 (*a*) S. Theis, A. Iturmendi, C. Gorsche, M. Orthofer, M. Lunzer, S. Baudis, A. Ovsianikov, R. Liska, U. Monkowius and I. Teasdale, *Angew. Chem., Int. Ed.*, 2017, **56**, 15857–15860; (*b*) Y. Liu, D. B. Turner, T. N. Singh, A. M. Angeles-Boza, A. Chouai, K. R. Dunbar and C. Turro, *J. Am. Chem. Soc.*, 2009, **131**, 26–27.

21 L. Agüero, L. G. Guerrero-Ramírez and I. Katime, *Mater. Sci. Appl.*, 2010, **1**, 103–108.

22 S. M. Zakeeruddin, Md. K. Nazeeruddin, R. Humphry-Baker and M. Grätzel, *Inorg. Chem.*, 1998, **37**, 5251–5259.

23 (*a*) O. Filevich, M. Salierno and R. Etchenique, *J. Inorg. Biochem.*, 2010, **104**, 1248–1251; (*b*) D. P. Nair, M. Podgorski, S. Chatani, T. Gong, W. Xi, C. R. Fenoli and C. N. Bowman, *Chem. Mater.*, 2014, **26**, 724–744; (*c*) L. Zayat, M. Salierno and R. Etchenique, *Inorg. Chem.*, 2006, **45**, 1728–1731.

24 (*a*) J. Li and D. J. Mooney, *Nat. Rev. Mater.*, 2016, **1**, 16071; (*b*) B. Thongrom, M. Dimde, U. Schedler and R. Haag, *Macromol. Chem. Phys.*, 2022, **224**, 2200271.

25 M. H. Shihan, S. G. Novo, S. J. Le Marchand, Y. Wang and M. K. Duncan, *Biochem. Biophys. Rep.*, 2021, **25**, 100916.

 This journal is © The Royal Society of Chemistry 2024